EMSP Project Annual Report

Project Title: **Atmospheric-Pressure Plasma Cleaning of Contaminated Surfaces**

DOE-ID Grant Number: **FG07-00ER45857**

EMSP project number: **73835**

Lead Principal Investigator:

Robert F. Hicks

Professor

UCLA Chemical Engineering

5531 Boelter Hall

Los Angeles, CA 90095-1592

(310) 206-6865

rhicks@ucla.edu

Co-Investigator:

Hans W. Herrmann

Los Alamos National Laboratory

Plasma Physics, P-24, MS E526

Los Alamos, NM 87545

(505) 665-6157

herrmann@lanl.gov

Graduate Students:

Xiawan Yang

Maryam Moravej

Gregory R. Nowling

UCLA Chemical Engineering

5531 Boelter Hall

Los Angles, CA 90095-1592

Research Objective

The objective of this work is to demonstrate a practical, atmospheric pressure plasma tool for the surface decontamination of radioactive waste. Decontamination of radioactive materials that have accumulated on the surfaces of equipment and structures is a challenging and costly undertaking for the US Department of Energy. Our technology shows great potential for accelerating this clean up effort.

Research Progress and Implications

This report summarizes the work accomplished during the third year of a three-year project. A low temperature, atmospheric pressure plasma has been developed with initial support from the Department of Energy, Environmental Management Sciences Program (see references). Now the goal is to characterize the reaction chemistry and demonstrate the viability of this technology on actual contaminated structures within the DOE complex. The reaction chemistry in the plasma and downstream region and the removal of uranium oxide from stainless steel surfaces has been investigated.

Plasma Physics

We have recently succeeded in breaking down argon at atmospheric pressure. It exhibits an intense white glow that is brighter than that observed with helium. We have investigated the current and voltage characteristics of pure argon and helium plasmas at 760 Torr. A SAES getter was installed in the feed lines to ensure that the impurity levels were less than 1 part per billion. Initially, both gases exhibit a Townsend dark region in which the voltage rises linearly with the current. The helium breaks down at about 200 V, whereas 500 V is required for argon. Thereafter, the normal glow regime is observed as shown in Fig. 1. For helium, this mode extends from 150 V and 0.5 A to 250 V and 1.0 A. By contrast, the normal glow for argon occurs over a very narrow range focused at 200 V and 0.75 A. Based on the IV measurements, the helium and argon plasma densities at 0.75 A are estimated to be 3.5 and 3.2 $x10^{11}$ cm^{-3}. In addition, the average electron temperatures are 1.3 and 0.3 eV, respectively.

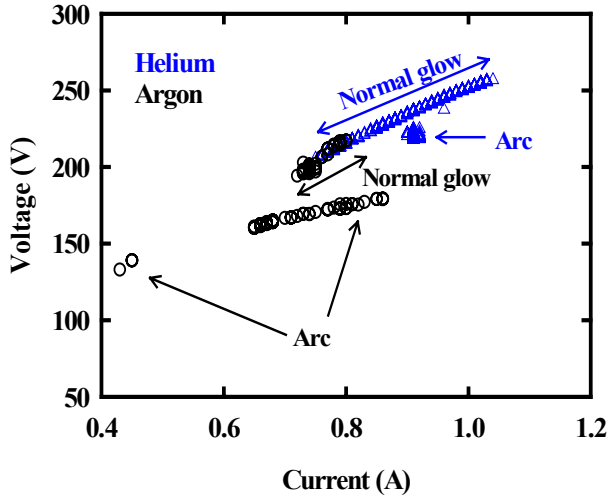

Fig. 1. Current-voltage curves for the normal glow region of helium and argon

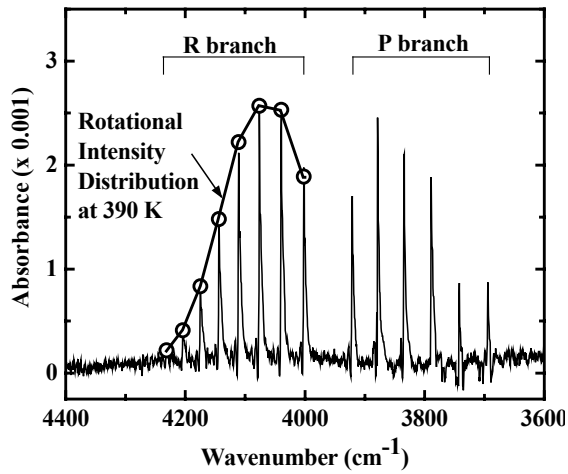

Fig. 2. Infrared spectrum of HF taken during the titration of F atoms with H_2 in the CF_4/He plasma afterglow.

Plasma Chemistry

We have measured the concentration of F atoms produced in a carbon tetrafluoride/helium discharge by titration with H_2 and by numerical modeling. Fluorine atoms rapidly react with H_2 to produce HF, which may be detected by infrared absorption spectroscopy. The plasma source employed in this work has been described in reference 3. Shown in Fig. 2 is the infrared spectrum of HF obtained by adding 0.7×10^{15} cm^{-3} H_2 to the afterglow of the plasma. The source was operated at 739.0 Torr He, 12.6 Torr CF_4, and 300 W RF power. We have used one of the peaks in the R branch to monitor the amount of HF produced in the titration experiments. The radio-frequency discharge produced 1.2×10^{15} cm^{-3} of F atoms, which was about two orders of magnitude higher than that found in low-pressure plasmas. A gas temperature of 117 °C was determined from the rotational intensity distribution of the R branch.

We have developed a numerical model to simulate the gas-phase reaction kinetics occurring in the discharge and the afterglow of the CF_4/He plasma. The reaction mechanism includes neutral species, ions, and electronically excited helium. The numerical model comprises the simultaneous set of material balances for these nineteen species. The average electron density and temperature in the plasma were estimated to be 6.1×10^{11} cm^{-3} and 2.5 eV from the measured discharge r.m.s. current and voltage.

Shown in Fig. 3 are the predicted densities of the ions and excited helium species in the discharge, assuming it was fed with 1.6 vol.% CF_4 in He at 760 Torr. The steady state densities of ions, He* and He^{2}* are achieved within 1.0 mm of the entering the plasma. The most abundant ions are CF_3^+, F^- and CF_3^-, which are in the range of 10^{12} to 10^{13} cm^{-3}. The total charge summed over all these ions and electrons equals zero, confirming that the plasma is neutral. It is further noted that F^- concentration is 3.0×10^{12} cm^{-3}, or about 5 times higher than the electron density. This indicates that the plasma is "electronegative," which is consistent with other studies of fluorine containing gas discharges.

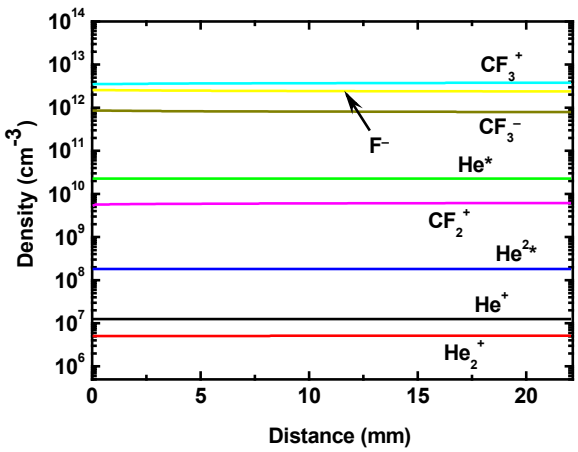

Fig. 3. Densities of ions and metastable helium in the CF_4/He plasma.

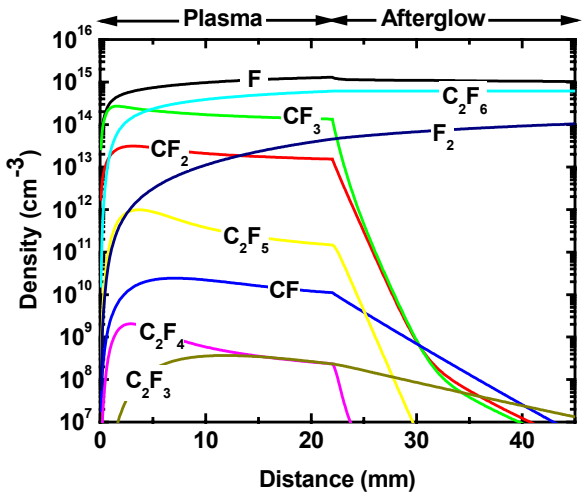

Fig. 4. Predicted profiles of the neutral species in the CF_4/He plasma and afterglow regions.

Presented in Fig. 4 are the predicted profiles of the neutral species in the plasma and in the afterglow downstream of the electrodes. The carbon tetrafluoride, whose density is 3.1×10^{17} cm^{-3}, is not shown in the figure. The CF_4 is dissociated in the plasma into F, CF_2 and CF_3. The CF_2 and CF_3 achieve concentrations in the range of 10^{13} and 10^{14} cm^{-3} inside the discharge, but are rapidly converted to C_2F_6 in the afterglow. By contrast, the concentration of F atoms rises to 1.1×10^{15} cm^{-3} inside the plasma, and then remains relatively constant over 20 mm downstream. This is because the F atoms are consumed by a three-body collision, $F + F + He \rightarrow F_2 + He$, which is a slow process at the plasma operating conditions. The F atom density predicted by the numerical simulation is in good agreement with the value measured by H_2 titration. This suggests that the numerical model is capturing the physics and chemistry of the process. According to the simulations, the active F atoms are generated primarily by impact with

metastable helium atoms, which are in turn produced by collision with the energetic electrons in the discharge.

Etching of Transuranic Elements

We have investigated the etching of uranium oxide with the atmospheric pressure plasma source. An etching rate of 4.0 μm/min has been observed at a sample temperature of 200 °C. Uranium oxide test samples were prepared by applying a solution of uranyl nitrate hexahydrate on stainless steel coupons. These samples were dried in air, and then baked for 5 hr at 700 °C. Each sample contained ~0.5 mg uranium. The plasma etching of UO_2 was performed with 15.0 Torr CF_4, 6.6 Torr O_2 and 729.0 Torr He, at 300 W RF power and 200 °C. Shown in Figs. 5 and 6 are scanning electron micrographs of samples before and after plasma etching for 2 min. It is found that the unprocessed sample is a porous thin film about 20.0 microns thick. Following 2 min of processing, the film is reduced to small aggregates 100 to 500 nm in length. This result shows that the reactive fluorine atoms penetrate into the layers, and strip the uranium from all the exposed surfaces. After 5 min of treatment, the porous film is removed, leaving behind a roughened steel surface.

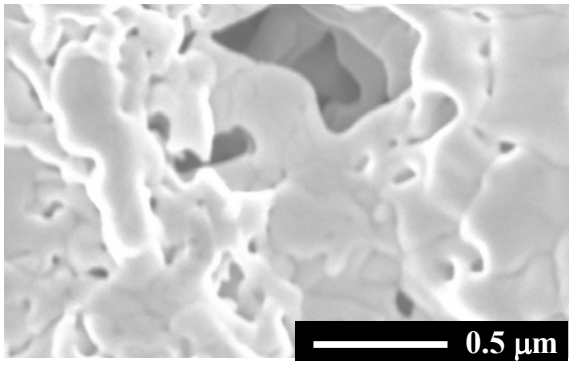

Fig. 5. Image of UO_2 film before etching.

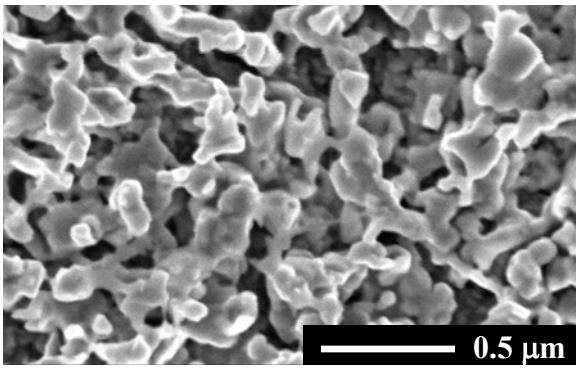

Fig. 6. Image of UO_2 film after a 2-min etch.

Shown in Fig. 7 are x-ray photoemission spectra of the U $4f_{5/2}$ and $4f_{7/2}$ states before and after etching the uranium oxide film. The U $4f_{7/2}$ peak for the fresh sample has a binding energy of 380.8 eV, which is indicative of the U^{+4} oxidation state (UO_2). After exposure to the plasma for 1 min, the 4f peaks shift more than 3.0 eV to higher binding energy due to uranium oxidation to U^{+6}. The intensities of photoemission peaks decrease rapidly with treatment, so that after 5 min, essentially all of the uranium has been removed. A plot of the integrated intensity of the U $4f_{7/2}$ band with process time is shown in Fig. 8. Over the first minute, the intensity increases

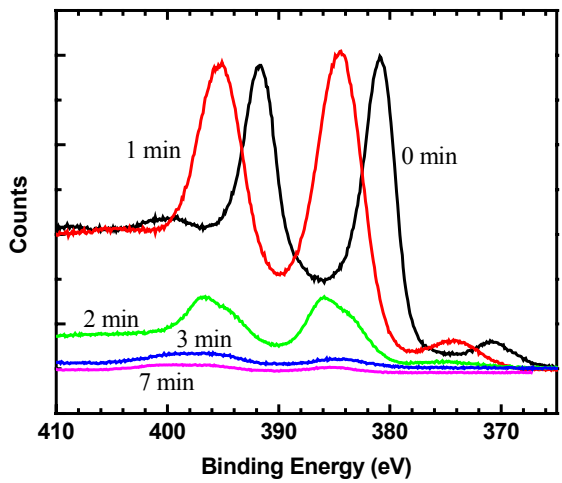

Fig. 7. XPS spectra of uranium oxide films before and after plasma etching.

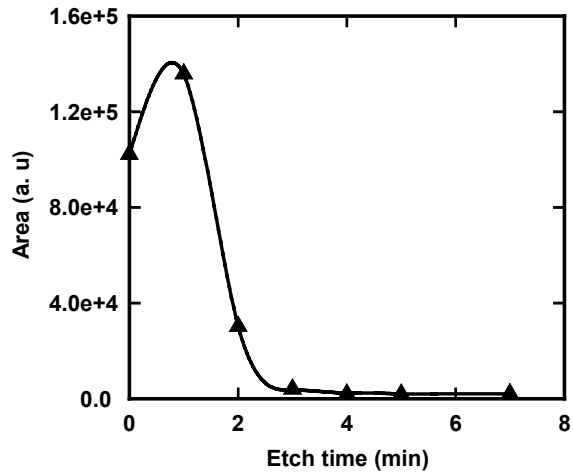

Fig. 8. Integrated intensity of the U $4f_{7/2}$ peak as a function of plasma etching time.

because the etching process initially increases the exposed surface area of the film (c.f. Fig. 6). Then the intensity rapidly decays as the UO_2 particles are stripped away.

Deconvolution of the U $4f_{7/2}$ band reveals that the film surface is converted primarily to uranium oxyfluorides in the U^{+6} oxidation state, i.e., UOF_4. It appears that the kinetically slow step in the overall process may be the reaction of gas-phase or adsorbed F atoms with the UOF_4 species to desorb UF_6. A surface reaction rate of 1.9×10^{15} molecules/cm^2·s has been estimated from the observed etching rate and the surface area of the film after exposure to the plasma. This reaction rate is about 100 times faster than that observed in other studies of actinide metal etching in low-pressure CF_4/O_2 plasmas.

Work on plutonium etching with the atmospheric pressure plasma system was to be carried out by the research team at Los Alamos National Laboratory, under Dr. Herrmann's direction. Please refer to his annual report for a description of the results achieved.

Planned Activities

We will further investigate the reaction chemistry of the CF_4-based atmospheric pressure plasma. The dependence of the concentration of reactive fluorine atoms on plasma operating conditions will be determined in order to optimize the etching rates of radioactive elements. Ultraviolet absorption and emission spectroscopy will be used to study the CF_x radicals. In addition, the effect of oxygen addition on the plasma chemistry will be assessed. By comparing

the experimental results with numerical models of the afterglow, we will be able to fully understand the reaction chemistry of the plasma decontamination system.

We will investigate the range of conditions for normal glow operation in the helium and argon discharges (flow rate, gap spacing, temperature, and RF power). The electron temperature and density will be measured directly from the plasma, and compared to the calculated values. Moreover, we will compare the rate of production of reactive fluorine atoms in helium and argon atmospheric pressure plasmas. If time permits, some preliminary experiments will be performed on air discharges containing CF_4.

Information Access

1. Yang, X., Babayan, S. E., and Hicks, R. F., "Measurement of the Fluorine Atom Concentration in a Carbon Tetrafluoride and Helium Atmospheric-Pressure Plasma," accepted by *Plasma Sources Sci. Technol*., on June 3, 2003.
2. Yang, X., Moravej, M., Babayan, S. E., Nowling, G., and Hicks, R. F., "Etching of Uranium Oxide with a Non-Thermal, Atmospheric Pressure Plasma," submitted to J. Nucl. Mater., on June 13, 2003
3. Babayan, S. E., Ding, G., Nowling, G. R., Yang, X., and Hicks, R. F., "Characterization of the Active Species in the Afterglow of a Nitrogen and Helium Atmospheric-Pressure Plasma," *Plasma Chem. Plasma Process.* **22***,* (2002), 255.
4. Park, J. Y., Henins, I., Herrmann, H. W., Selwyn, G. S., and Hicks, R. F., "Discharge Phenomena of an Atmospheric Pressure Radio-Frequency Capacitive Plasma Source," *J. of App. Phys.*, **89**, (2001), 20.
5. Park, J. Y., Henins, I., Herrmann, H. W., and Selwyn, G. S., "Gas Breakdown in an Atmospheric Pressure RF Capacitive Plasma Source," *J. of App. Phys.*, **89**, (2001), 15.
6. Babayan, S. E., Ding, G., and Hicks, R. F., "Determination of the Nitrogen Atom Density in the Afterglow of a Nitrogen and Helium, Non-Equilibrium, Atmospheric Pressure Plasma," *Plasma Chem. Plasma Process.* **21**, (2001), 505.

7. Babayan, S. E., Jeong, J. Y., Schütze, A., Tu, V. J., Moravej, M., Selwyn, G. S., and Hicks, R. F., "Deposition of Silicon Dioxide Films with a Non-Equilibrium Atmospheric-Pressure Plasma Jet," *Plasma. Sources. Sci. Technol.* **10**, (2001), 573.

8. Park, J. Y., Henins, I., Herrmann, H. W., and Selwyn, G. S., "Neutral Bremsstrahlung Measurement in an Atmospheric-Pressure Radio-Frequency (RF) Discharge," *Physics of Plasmas*, **7**, (Aug 2000), 3141.

9. Tu, V. J., Jeong, J. Y., Schütze, A., Babayan, S. E., Selwyn, G. S., Ding, G., and Hicks, R. F., "Tantalum Etching with a Non-Thermal Atmospheric-Pressure Plasma," *J. Vac. Sci. Technol. A* **18**, (2000), 2799.

10. Park, J. Y., Henins, I., Herrmann, H. W., Selwyn, G. S., Jeong, J. Y., Hicks, R. F., Shim, D., and Chang, C. S., "An Atmospheric Pressure Plasma Source," *App. Phys. Lett.*, **76**, (Jan 2000), 288.

11. Jeong, J. Y., Park, J. Y., Henins, I., Babayan, S. E., Tu, V. J., Selwyn, G. S., Ding, G., and Hicks, R. F., "Reaction Chemistry in the Afterglow of an Oxygen-Helium, Atmospheric-Pressure Plasma," *J. Phys. Chem.*, **104**, (2000), 8027.

12. Jeong, J. Y., Babayan, S. E., Schütze, A., Tu, V. J., Park, J. Y., Henins, I., Selwyn, G. S., and Hicks, R. F., "Etching polyimide with a non-equilibrium atmospheric-pressure plasma jet," *J. Vac. Sci. Technol. A* **17**, (1999), 2581.

13. Jeong, J. Y., Babayan, S. E., Tu, V. J., Henins, I., Velarde, J., Selwyn, G. S., and Hicks, R. F., "Etching Materials with an Atmospheric-Pressure Plasma Jet," *Plasma Sources Sci. and Tech.* **7**, (1998), 282.

14. Babayan, S. E., Jeong, J. Y., Tu, V., Selwyn, G. S., and Hicks, R. F., "Deposition of Glass Films with an Atmospheric-Pressure Plasma Jet," *Plasma Sources Sci. and Tech.* **7**, (1998), 286.

15. Schütze, A., Jeong, J. Y., Babayan, S. E., Park, J., Selwyn, G. S., and Hicks, R. F., "The Atmospheric-Pressure Plasma Jet: A Review and Comparison to other Plasma Sources," *IEEE Trans. Plasma Sci.* **26**, (1998), 1685.

16. http://www.seas.ucla.edu/prosurf/